

Supplementary Information

**Carbon Dots with Efficient Solid-State Photoluminescence towards White  
Light-Emitting Diodes**

*Jinyang Zhu, Xue Bai, Yue Zhai, Xu Chen, Yongsheng Zhu, Gencai Pan, Hanzhuang Zhang,  
Biao Dong, and Hongwei Song*

**Experimental Section**

**Materials.**

All reagents were used as received without further purification. Dimethylformamide (DMF), citric acid and urea were purchased from Beijing Chemical Works. Hexadecyltrimethyl ammonium bromide (CTAB), decyltrimethylammomium bromide, dodecyltrimethylammonium bromide, cetyltrimethylammonium chloride (CTAC), polyvinylpyrrolidone (PVP, K90) were purchased from Sigma-Aldrich.

**Preparation of pristine CDs.**

1 g citric acid and 2 g urea were firstly dissolved in 10 ml of DMF, then the solution was transferred into a poly(tetrafluoroethylene)-lined autoclave and sealed carefully. The autoclave was heated at 180 °C for 8 h. After that, a dark brown solution was centrifuged and washed thoroughly with water. The precipitate was collected, dissolved in water.

**Preparation of CD-10, CD-12, and CD-CTAB.**

250 mg of CTAB, decyltrimethylammomium bromide (10-carbon alkyl), and dodecyltrimethylammonium bromide (12-carbon alkyl) were respectively dissolved in 10 ml water and stirred for 5 min at 50 °C. Then took 0.5 mL the obtained transparent solutions and mixed with 5 mL pristine CDs solution, named CD-CTAB, CD-10 and CD-12, respectively.

### **Preparation different concentration of CTAB to modify the pristine CDs.**

100 mg, 200 mg, 250 mg or 300 mg of CTAB were dissolved in 10 ml water, respectively, stirred for 5 min at 50 °C. Then took 0.5 mL the obtained transparent solution and mixed with 5 mL CD solution. Then CD solutions modified with different concentration of CTAB were obtained.

### **Preparation of CD-CTAB-K90.**

1 g PVP-K90 was added slowly to the CD-CTAB solution under vigorous stirring around 1 h until it transformed to a sticky and bubble mixture. Then spreaded the mixture on a quartz glass and dried for 1 h at 50 °C. The CD-CTAB-K90 film was obtained.

### **Preparation of CD-CTAB powder.**

5 mL of CD-CTAB solution was directly dried at 50 °C and produced solid-state CD-CTAB powder, named S-CD-CTAB.

### **Preparation of PVP-CD films: S<sub>1</sub>, S<sub>2</sub>, S<sub>3</sub>, S<sub>4</sub>.**

100 mg, 200 mg, 250 mg or 300 mg of CTAB were dissolved in 10 ml water, respectively. Then took 0.5 mL the obtained transparent solution and mixed with 5 mL pristine CDs solution. 1 g of PVP-K90 was added slowly to the CD-CTAB solution under vigorous stirring around 1 h until it transformed to a sticky and bubble mixture. Then spreaded the mixture on a quartz glass and dried for 1 h at 50 °C. The films were named as S<sub>1</sub>, S<sub>2</sub>, S<sub>3</sub>, or S<sub>4</sub>.

### **Characterization techniques.**

Field emission scanning electron microscope (FE-SEM) investigations were carried out using a JEOL JSM-7500 operated at an accelerating voltage of 15 kV. For the transmission electron microscopy (TEM) and high-resolution microscopy measurements, one or two drops of the as-prepared sample solutions were deposited on a copper grid coated with an amorphous carbon film. The images were recorded with a JEOL-2100F microscope with a field emission gun operated at an accelerating voltage of 200 kV. The Raman spectra were investigated by using a Horiba Jobin Yvon Xplora spectrometer under an excitation of 532 nm. X-ray photoelectron spectroscopy (XPS) was performed with an ESCALab220i-XL electron spectrometer from VG Scientific. Fourier transformed infrared (FT-IR) spectra were recorded with a Nicolet 6700 FT-IR spectrometer. The pellets were prepared by adding 1-2 mg of CTAB, CDs and CD-CTAB powder to 100 mg of KBr. The mixture was carefully homogenized and compressed with a uniaxial pressure of 9 MPa.

### Optical studies.

Ultraviolet-visible (UV-Vis) absorption spectra were measured with a Shimadzu UV-3101PC UV-Vis scanning spectrophotometer. Photoluminescence spectra were recorded at room temperature by using one FLS980 spectrometer (Edinburgh). The excitation source was a 450W Xe arc lamp. The time-resolved emission decay curves were measured at room temperature with a PLS980 time correlated single-photon counting (TCSPC) system.

The absolute emission quantum yield values were measured at room temperature using a commercial integrating sphere installed in FLS980 spectrometer (Edinburgh). The emission quantum yield ( $\Phi$ ) is given by <sup>[1]</sup>

$$\Phi = \frac{N_{emi}}{N_{abs}} = \frac{\int_{\lambda_1}^{\lambda_2} \frac{\lambda}{hc} [I_{em}^{sample}(\lambda) - I_{em}^{reference}(\lambda)] d\lambda}{\int_{\lambda_3}^{\lambda_4} \frac{\lambda}{hc} [I_{ex}^{sample}(\lambda) - I_{ex}^{reference}(\lambda)] d\lambda}$$

Where  $N_{emi}$  and  $N_{abs}$  are the number of photons absorbed and emitted by a sample, respectively,  $h$  is Planck's constant,  $c$  is the velocity of light,  $I_{em}^{sample}$  and  $I_{em}^{reference}$  are the emission intensities of the measured with and without a sample respectively, in the emission spectra wavelength interval  $[\lambda_1, \lambda_2]$ ,  $I_{ex}^{sample}$  and  $I_{ex}^{reference}$  are the intensities of the excitation radiation measured with and without a sample respectively, in the excitation wavelength interval  $[\lambda_3, \lambda_4]$ . In order to validate the calculation methodology, the commercial YAG:Ce<sup>3+</sup> (BM302D, Jiangsu Bree Optronics Co., Ltd., peaking at 551 nm) was measured under the same experimental conditions. The QY value for YAG:Ce<sup>3+</sup> was measured to be 88% excited at 460 nm. The repeated measurement was also performed for each sample revealing a standard deviation below 0.5 %. The measurement accuracy is within 10% according to the manufacturer.

### Thermal stability test.

The thermal stability of CD-CTAB solution and CD-CTAB-K90 solid-state film samples were measured by FLS980 spectrometer. The temperature of the samples were controled by the equiment (temperature programming, Optistat DN-2, MercuryiTC). For the CD-CTAB aqueous solution, the thermal stability of the emission spectra was investigated in the temperature range from 25 to 95 °C (each 15 °C ) and for CD-CTAB-K90 solid-state film, the emission spectra was investigated in the temperature range from 25 to 150 °C (each 25 °C).

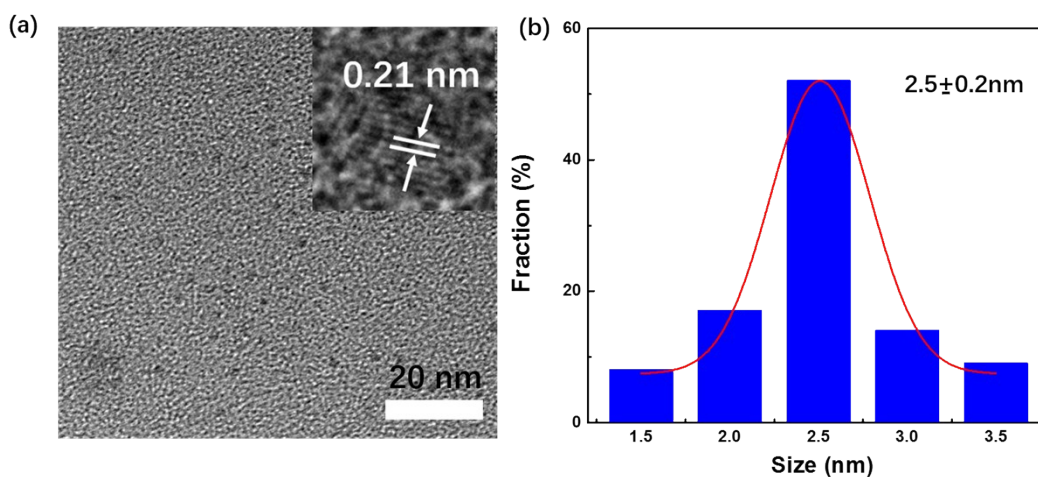


**Figure S1. (a) The TEM image and (b) size distribution image of pristine CDs; the inset of (a) shows a HRTEM image of a dot. It shows the diameter of pristine CDs with a uniform size distribution around 2.5 nm. HRTEM image reveals the pristine CDs have crystallinity of graphite core with lattice spatial of 0.21 nm, the same as that of (100) in-plane within graphite, indicating a graphite nature of backbone in the pristine CDs.<sup>[2]</sup>**

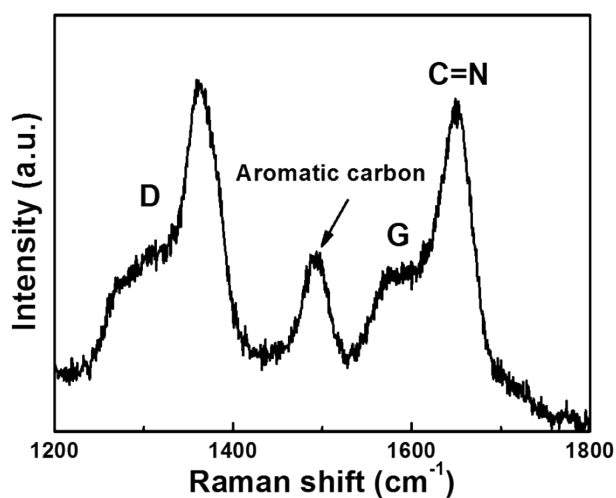


**Figure S2. Raman spectrum of pristine CDs under the excitation of 532 nm laser. Common features were observed in the 1200-1800 cm<sup>-1</sup> region, where the G band originates from graphitic sp<sup>2</sup> carbon and D band indicates the existence of disorder structures or defects in the CDs. Beside the D band and G band, strong signals assigned to C=N and aromatic carbon.<sup>[3]</sup>**

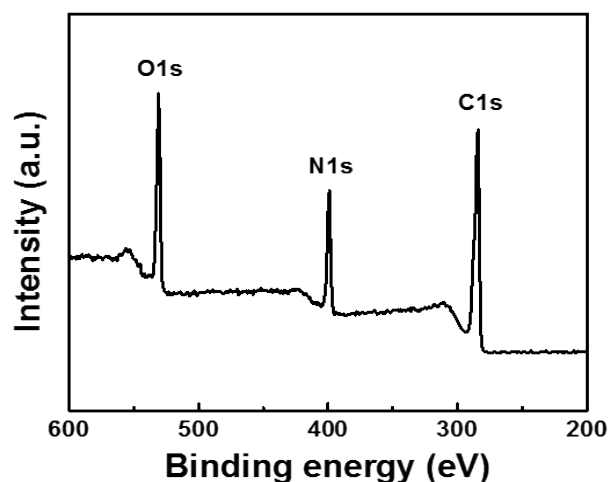


**Figure S3. XPS spectrum of pristine CDs.** XPS measurement were carried out to determine the actual compositions of the prepared pristine CDs sample. O1s, N1s and C1s peaks at 531 eV, 400 eV and 284 eV, respectively, are observed in the XPS full survey spectra. Nitrogen is detected by N1s signal indicating the successful nitrogen-doping into the pristine CDs.<sup>[4]</sup>

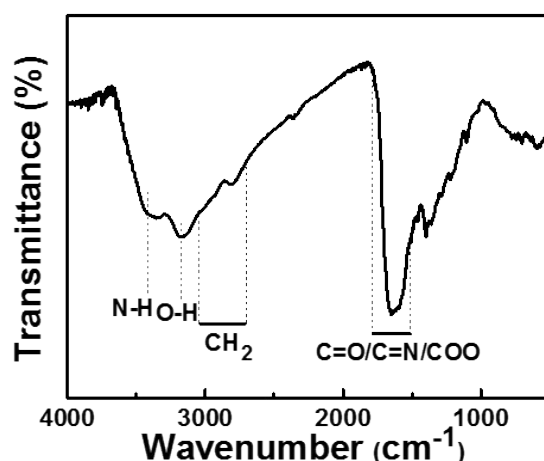


**Figure S4. FT-IR spectrum of pristine CDs.** FT-IR spectrum reveals that pristine CDs possessed abundant hydrophilic groups such as the stretching vibration of O-H and stretching vibration of N-H at 3050-3650 cm<sup>-1</sup>.<sup>[3b]</sup> The broad band from 1600-1750 cm<sup>-1</sup> encompasses three vibrations: the stretching vibrations of C=O at 1719 cm<sup>-1</sup> in carboxyl and C=N at 1665 cm<sup>-1</sup> in CNH group, as well as the stretching of C=O at 1636 cm<sup>-1</sup> in amide, which suggests the formation of O/N-related surface state on the surface of the as-prepared CDs.<sup>[5]</sup>

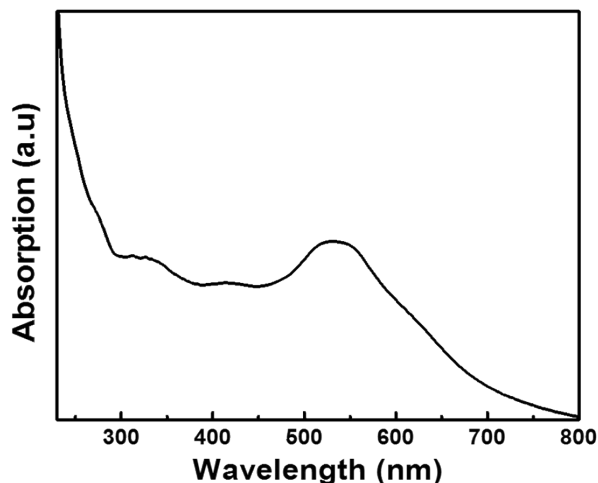


**Figure S5. The UV-Vis absorption of pristine CDs aqueous solution.** The absorption at 260 nm and 350 nm are the intrinsic absorption peak of carbon cores which are assigned to the  $\pi \rightarrow \pi^*$  transition and the  $n \rightarrow \pi^*$  transitions, respectively.<sup>[3a]</sup> Meanwhile, a broad tail peak of the  $n \rightarrow \pi^*$  absorption appears at 340-420 nm, which can be attributed to the overlap of the intrinsic absorption and the surface state absorption of C=O groups.<sup>[3]</sup> In addition, the C=N groups of the surface state absorption peak is found in *ca.* 530 nm.<sup>[3b]</sup>

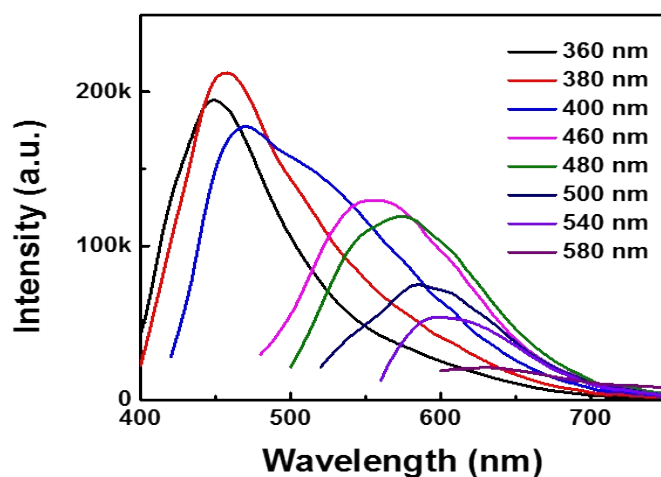


**Figure S6. Emission spectra of pristine CDs aqueous solution excited at different wavelengths.** The emission spectra of the as-prepared pristine CDs show an excitation-dependent feature with red-shift of photoluminescence emission as the excitation wavelength increases from 360 nm to 580 nm.

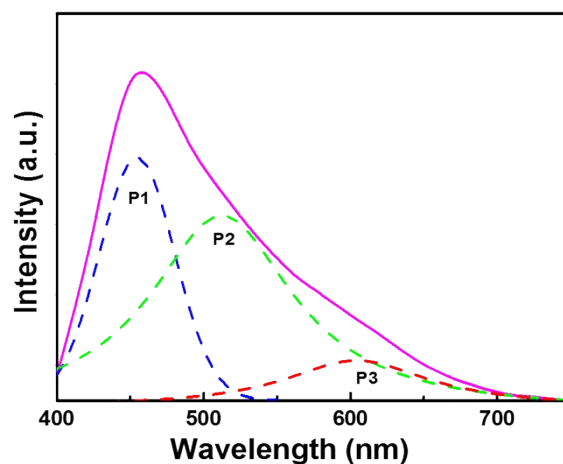


**Figure S7. Emission spectra of pristine CDs aqueous solution excited at 380 nm.** The emission spectra of pristine CDs excited under 380 nm wavelength can be fitted by three components: P1 is dominated by blue emission, P2 and P3 are in green and red regions, respectively. Consistent with the previous studies, the blue emitting component can be associated to intrinsic state emission of carbogenic core, and the excitation dependence of green and red emitting components are dominated by the C=O and C=N surface states, respectively.<sup>[3b,6,7]</sup>

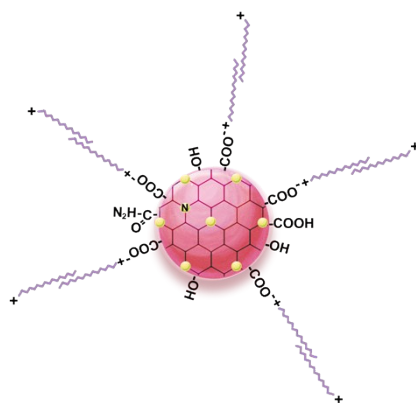


**Figure S8. Schematic illustration of the structure of CD-CTAB in water.** The transform of Zeta potential from negative value of  $-18.7$  mV in pristine CDs to positive value of  $+37.3$  mV in CD-CTAB suggesting a bilayer structure of CTAB molecular formed on the surface of pristine CDs, which is similar to the previous reports for the gold nanoparticles.<sup>[8]</sup> The CTAB bilayer consists of two surfactant leaflets; one is associated with the pristine CDs surface via the quaternary ammonium head groups, and the other has the surfactant head groups facing the aqueous media. This bilayer assembly is energetically favored as it guarantees hydrophobic interactions between the surfactant tails in the bilayer core and hydrophilic interactions of the charged head group with the pristine CDs or aqueous solution.

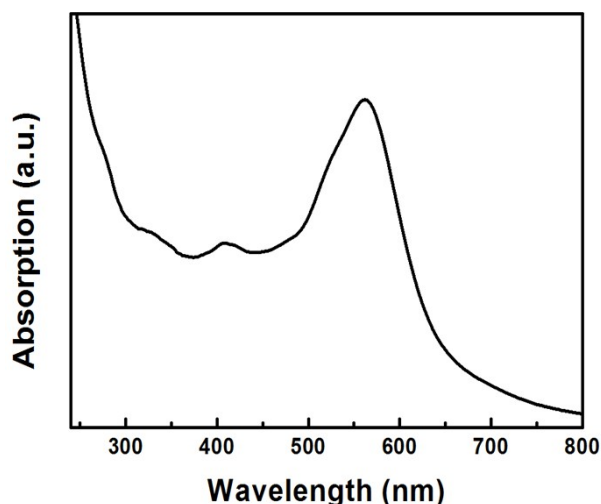


**Figure S9.** The UV-Vis absorption of CD-CTAB aqueous solution.

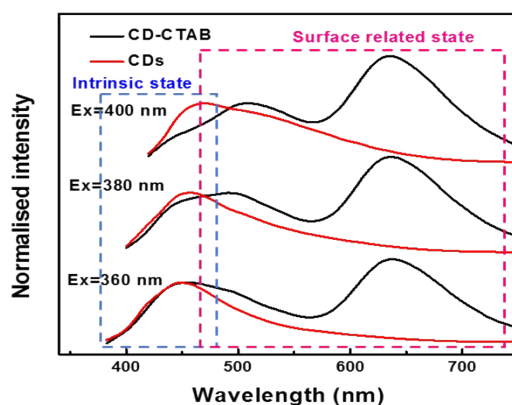


**Figure S10.** Emission spectra excited at 360, 380, and 400 nm for the pristine CDs and CD-CTAB aqueous solution. Under excitation from 360 to 400 nm, the pristine CDs show one main emission component at blue green spectral region and a weak emitting tail spanning to 650 nm, while the CD-CTAB reveals the presence of wide emission bands spanning the whole visible spectral region, in which three-primary chromatic components at *ca.* 450, 510 and 640 nm overlapped with each other resulting in a large broad band. The blue emission can be related to the intrinsic state emission of carbogenic core, and the green and red emissions are dominated by the C=O and C=N surface states, respectively. <sup>[3b,6,7]</sup>

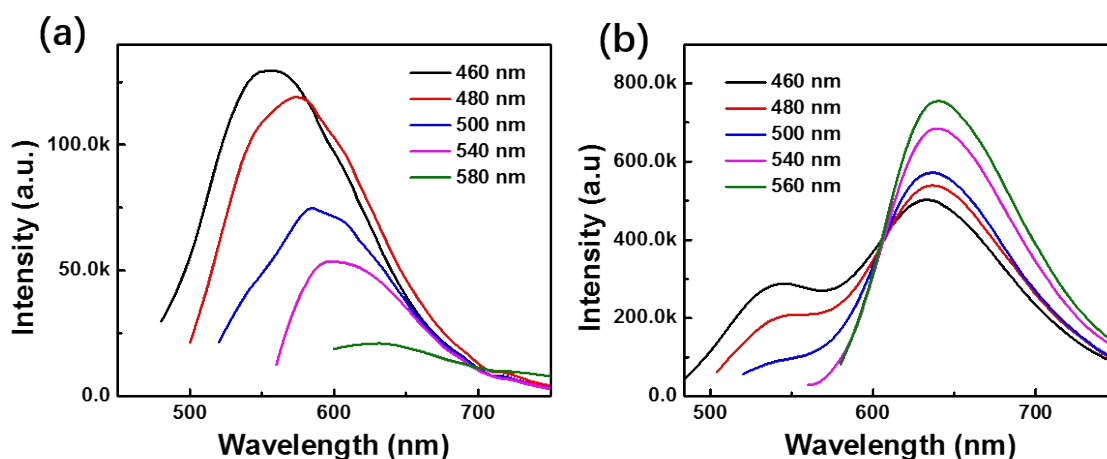


**Figure S11.** Emission spectra of a) The pristine CDs aqueous solution, and b) the CD-CTAB aqueous solution, under the excitation from 460 to 580 nm. Under the excitation from 500 to 580 nm, the emissions of pristine CDs decrease in the intensities and shift to red. Differing from the pristine CDs, CD-CTAB shows two emission bands, one is in green region and the other one is in red region. With increased excitation wavelengths, the green emission disappears gradually, the red emission is excitation-independent and keeps its position at *ca.* 640 nm and increases in intensities.

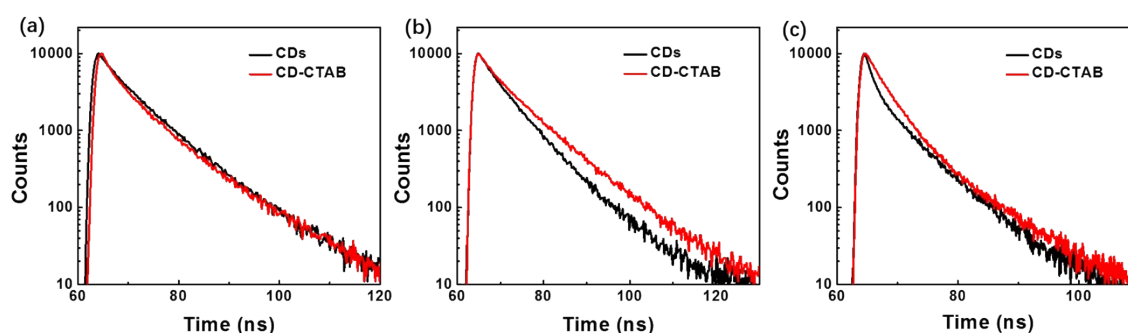


**Figure S12.** Fluorescence decay curves of pristine CDs and CD-CTAB recorded at emission wavelengths of 450 (a), 500 (b) and 620 nm (c), in water. The average lifetime values measured at blue emission band of CD-CTAB is similar to the pristine CDs, while the lifetime values measured for the green and red components of CD-CTAB are substantially longer than those of pristine CDs. The values increase (26%) from 7.0 ns to 8.8 ns as monitoring green emission, and increase (17%) from 5.1 ns to 5.9 ns for the red emission.

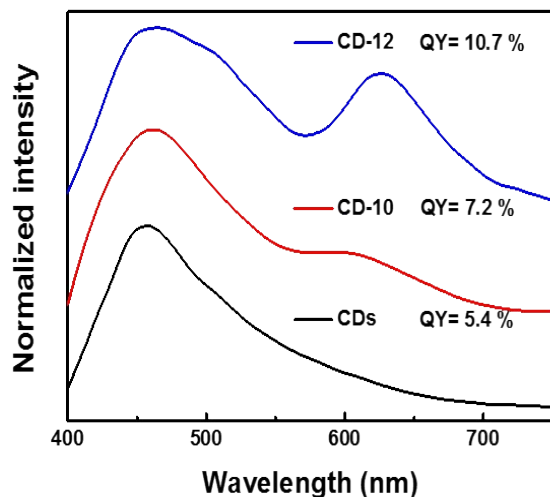


Figure S13. Emission spectra of pristine CDs, CD-10, and CD-12 aqueous solutions excited at 380 nm (normalized at 450 nm).

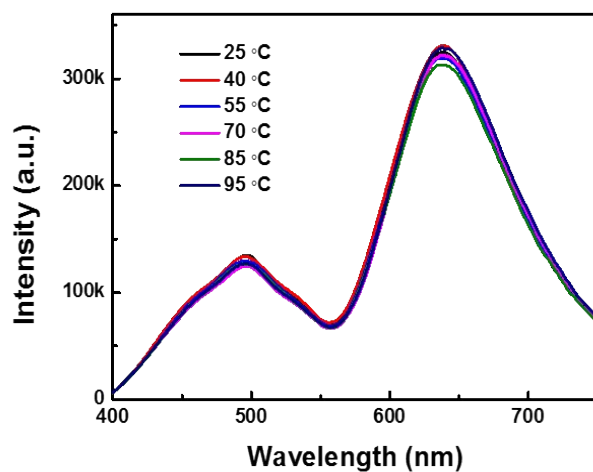
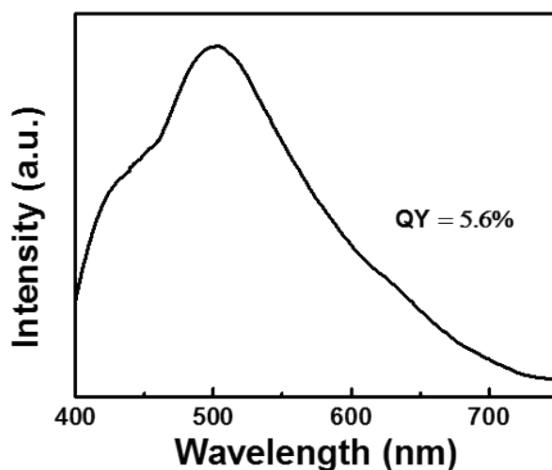
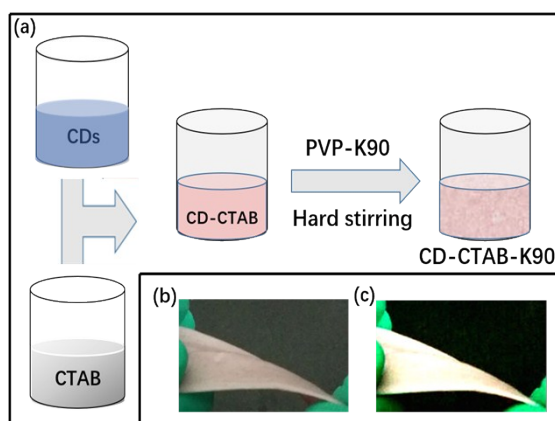


Figure. S14 Emission spectra of CD-CTAB aqueous solution at different temperatures (380 nm excitation).



**Figure S15. Emission spectra of CD-CTAB dried into solid state excited at 380 nm.** The emission spectra of CD-CTAB reveals an obviously change of distribution of emitting energy and decrease of QY compared with CD-CTAB aqueous solution (12.7%), suggesting that solid-state quenching occurred.



**Figure S16. Preparation of white-light-emitting CD-CTAB-K90 solid-state film (a), and the photographs of CD-CTAB-K90 film under daylight (b) and 365 nm of UV light (c).**

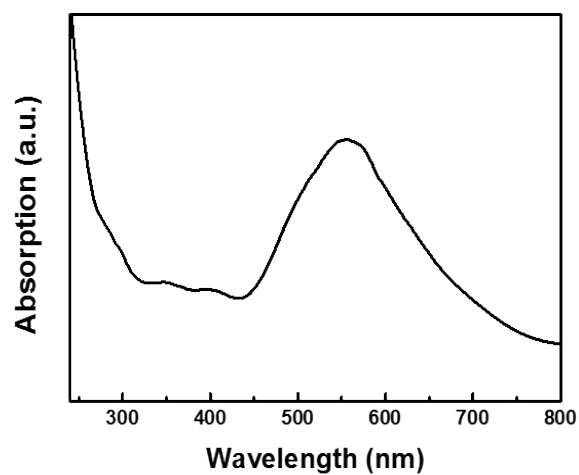


**Figure S17.** The UV-Vis absorption of CD-CTAB-K90 solid-state film.

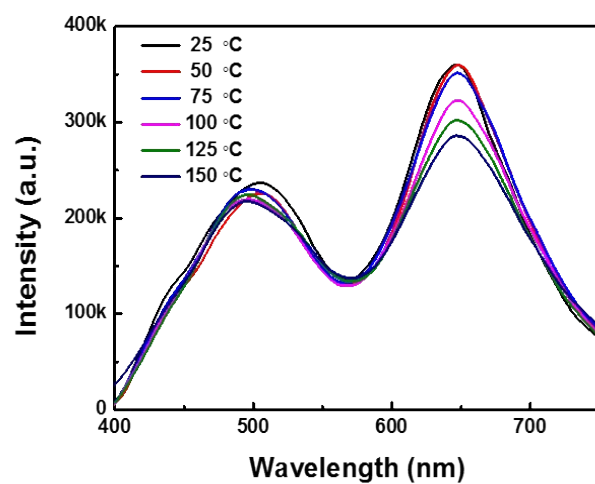


**Figure S18.** Emission spectra of CD-CTAB-K90 solid-state film at different temperatures (380 nm excitation).

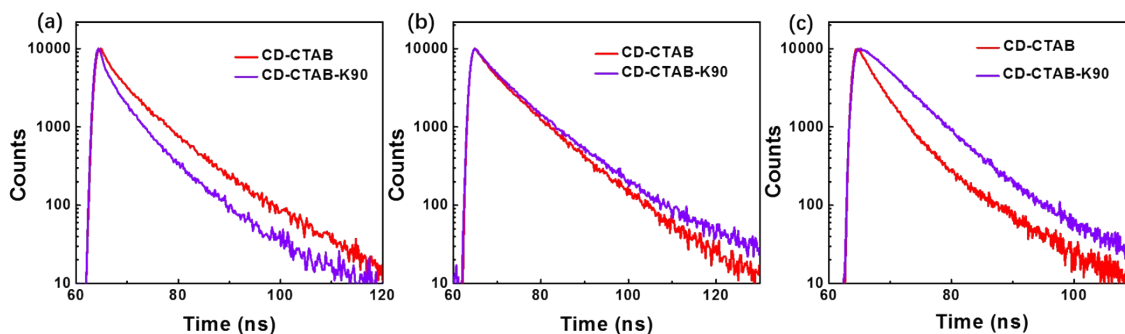


**Figure S19. Fluorescence decay curves of CD-CTAB aqueous solution and CD-CTAB-K90 solid-state film recorded at emission wavelengths of 450 (a), 500 (b) and 640 nm (c).** The average lifetime values measured at blue emission of CD-CTAB-K90 solid-state film decreases obviously comparing with the CD-CTAB aqueous solution; while the average lifetime values measured at the green and red emitting components of CD-CTAB-K90 solid-state film are substantially larger than those acquired in the CD-CTAB aqueous solution.

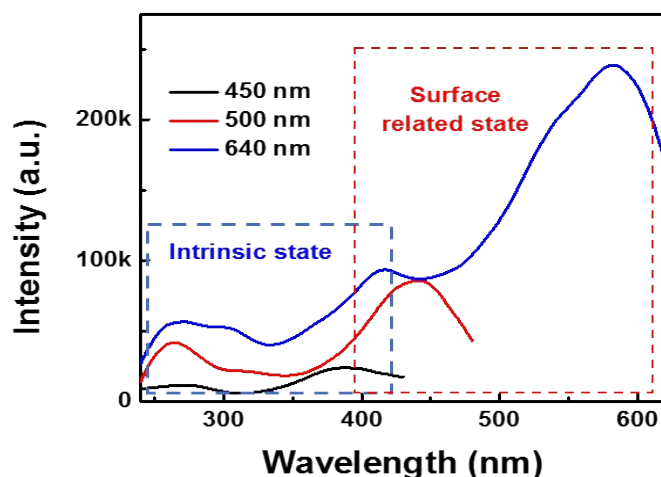


**Figure S20. The excitation spectra of CD-CTAB-K90 solid-state film monitoring at blue (450 nm), green (500 nm) and red emission (640 nm), respectively.** It is notable that when monitoring at blue emission, it shows two broad components from 240 to 300 nm and 350 to 400 nm in the UV spectral region, respectively, which can be ascribed to the intrinsic state of carbogenic core.<sup>[3]</sup> When monitoring at green and red emitting components, besides a broad band in visible spectral region which is ascribed to the surface states, the two components associated to intrinsic state also can be detected. Therefore, we propose that the main excitation path in UV region for the green and red emissions is through the energy transfer of excited electrons in the state of intrinsic  $sp^2$  domains.

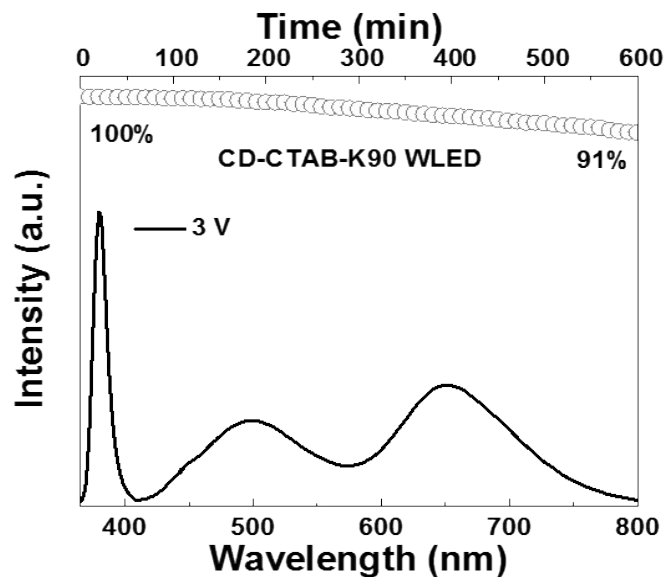


Figure S21. Emission spectrum (bottom) of the CD-CTAB-K90 based WLED operated at forward voltage of 3 V, and its emission intensity stability in 10 h.

Table S1. The photoluminescence QYs of CDs, CD-10, CD-12 and CD-CTAB aqueous solution under excitation of 380 nm.

Sample	CDs	CD-10	CD-12	CD-CTAB
QY	5.4 %	7.2 %	10.7 %	12.7 %

Table S2. The zeta potentials of CDs, CD-10, CD-12 and CD-CTAB aqueous solution.

Sample	CDs	CD-10	CD-12	CD-CTAB
Zeta potential	-17.2 mV	31.3 mV	33.7 mV	37.3 mV

Table S3. The CIE and CCT values of S<sub>1</sub>, S<sub>2</sub>, S<sub>3</sub> and S<sub>4</sub>.

Sample	S <sub>1</sub>	S <sub>2</sub>	S <sub>3</sub>	S <sub>4</sub>
CIE	(0.33,0.33)	(0.35, 0.31)	(0.38, 0.32)	(0.41,0.31)
CCT	5136K	4843K	3631K	2946K

### **Note S1. TEM, Raman, XPS, FT-IR and AFM data of pristine CDs**

The transmission electron microscopy (TEM) image in Figure S1 shows the pristine CDs with a narrow size distribution. Besides the presence of a carbogenic core, the non-crystalline region on the edges of the particle suggest that the pristine CDs also possess abundant surface chemical groups or defects (HRTEM).<sup>[9]</sup> These results were further confirmed by Raman spectroscopy as illustrated by Figure S2. Common features were observed in the 1200-1800  $\text{cm}^{-1}$  region, where the G band (1551-1560  $\text{cm}^{-1}$ ) as well as the band of aromatic carbon (1500  $\text{cm}^{-1}$ ) confirmed the existence of the  $\text{sp}^2$  hybridized crystalline core, and the D band located at around 1340-1348  $\text{cm}^{-1}$  accounts for defects associated with amorphous carbon or surface dangling bond. Beside the D band and G band, strong signals assigned to C=N and aromatic carbon.<sup>[3]</sup> Moreover, the intensity ratio of  $I_D/I_G$  is normally to calculate the quality of crystalline quality of pristine CDs. The high  $I_D/I_G$  ratio indicated that large amount of disorder or amorphous carbon existed within pristine CDs, which result from the doping with heteroatoms of N atoms.<sup>[6]</sup> X-ray photoelectron spectroscopy (XPS) measurements were carried out to determine the actual compositions of the pristine CDs sample. As can be seen in Figure S3, the results show three peaks at  $\sim 531$  eV, 400 eV and 284 eV, which are attributed to O1s, N1s and C1s, respectively. Nitrogen is detected by N1s signal indicating the successful of nitrogen-doping into the pristine CDs.<sup>[4]</sup> FT-IR spectra in Figure S4 reveal that pristine CDs samples possessed abundant hydrophilic groups such as the stretching vibration of O-H and stretching vibration of N-H at 3050-3650  $\text{cm}^{-1}$ .<sup>[2b]</sup> The broad band from 1600-1750  $\text{cm}^{-1}$  encompasses three vibrations: the stretching vibrations of C=O at 1719  $\text{cm}^{-1}$  in carboxyl and C=N at 1665  $\text{cm}^{-1}$  in CNH group, as well as the stretching of C=O at 1636  $\text{cm}^{-1}$  in amide, which suggests the formation of O/N-related surface state on the surface of the as-prepared CDs.<sup>[5]</sup>

## Note S2. Discussion of the optical properties of pristine CDs

The UV-vis absorption of pristine CDs (Figure S5) shows a broad absorption spectrum with a gradual change up to 700 nm. The absorption at 260 nm and 350 nm are the intrinsic absorption peaks which are assigned to the  $\pi \rightarrow \pi^*$  and the  $n \rightarrow \pi^*$  transitions, respectively.<sup>[3a]</sup> Meanwhile, a broad tail peak of the  $n \rightarrow \pi^*$  absorption appears at 340-420 nm, which are attributed to the overlap of the intrinsic absorption and the surface state absorption of C=O groups.<sup>[3]</sup> The C=N groups of the surface state absorption peak is found in the *ca.* 530 nm.<sup>[3a]</sup> The unusually broad absorption band (particularly in the visible-light region) demonstrates the presence of multiple electronic absorption transitions.<sup>[6]</sup> The pristine CDs present tunable emission features depending on excitation wavelength from blue to red wavelength region shown in Figure S6, which is due to the multiple emission origins existed in the pristine CDs rather than a wide distribution of size. It is notable that the photoluminescence (PL) spectra of pristine CDs show broad emission under relatively high energy excitation lights (360-400 nm), demonstrating the as-produced emissions might behave as excitation lights and thus inducing multiple emissions.<sup>[6]</sup> The PL spectra which excited under 380 nm (Figure S7) can be fitted by 3 peaks: P1 is at blue emission region, P2 is at green emission region and P3 is at red emission region. From the previous reports, the blue emission band at around 450 nm are normally associated to intrinsic state emission of carbogenic core, while the green and red ones are associated to C=O and C=N related surface states. <sup>[3b,6,7]</sup> Therefore, the emission from pristine CDs are resulting from the cooperation of intrinsic and surface states synchronously.

## References

- 1 X. Bai, G. Caputo, Z. D. Hao, V. Freitas, J. H. Zhang, R. L. Longo, O. L. Malta, R. A. S. Ferreira and N. Pinna, *Nature Commun.* 2014, **5**, 5702.
- 2 a) Y. Chen, M. Zheng, Y. Xiao, H. Dong, H. Zhang, J. Zhuang, H. Hu, B. Lei and Y. Liu, *Adv. Mater.*, 2016, **28**, 312; b) S. Qu, D. Zhou, D. Li, W. Ji, P. Jing, D. Han, L. Liu, H. Zeng and D. Shen, *Adv. Mater.*, 2016, **28**, 3516; c) S. Zhu, J. Shao, Y. Song, X. Zhao, J. Du, L. Wang, H. Wang, K. Zhang, J. Zhang and B. Yang, *Nanoscale*, 2015, **7**, 7927; d) Y. Wang, S. Kalytchuk, L. Wang, O. Zhovtiuk, K. Cepe, R. Zboril and A. L. Rogach, *Chem. Commun.*, 2015, **51**, 2950.
- 3 a) C. J. Reckmeier, J. Schneider, A. S. Susha and A. L. Rogach, *Opt. Express*, 2016, **24**, A312; b) D. Chen, W. Wu, Y. Yuan, Y. Zhou, Z. Wan and P. Huang, *J. Mater. Chem. C*, 2016, **4**, 9027.
- 4 a) H. Ding, S. Yu, J. Wei and H. Xiong, *ACS Nano*, 2015, **10**, 484; b) D. Li, D. Han, S. Qu, L. Liu, P. Jing, W. Ji, X. Wang, T. Zhang and D. Shen, *Light: Sci. Appl.*, 2016, **5**, e16120.
- 5 a) S. Sun, L. Zhang, K. Jiang, A. Wu and H. Lin, *Chem. Mater.*, 2016, **28**, 8659; b) H. Li, X. He, Z. Kang, H. Huang, Y. Liu, J. Liu, S. Lian, C. A. Tsang, X. Yang and S. T. Lee, *Angew. Chem. Int. Ed.*, 2010, **49**, 4430.
- 6 L. Pan, S. Sun, A. Zhang, K. Jiang, L. Zhang, C. Dong, Q. Huang, A. Wu and H. Lin, *Adv. Mater.*, 2015, **27**, 7782.
- 7 S. Zhu, J. Zhang, S. Tang, C. Qiao, L. Wang, H. Wang, X. Liu, B. Li, Y. Li, W. Yu, X. Wang, H. Sun and B. Yang, *Adv. Funct. Mater.*, 2012, **22**, 4732.
- 8 C. J. Murphy, L. B. Thompson, A. M. Alkilany, P. N. Sisco, S. P. Boulos, S. T. Sivapalan, J. A. Yang, D. J. Chernak and J. Y. Huang, *J. Phys. Chem. Lett.*, 2010, **1**, 2867.
- 9 K. A. S. Fernando, S. Sahu, Y. Liu, W. K. Lewis, E. A. Gulians, A. Jafariyan, P. Wang, C. E. Bunker and Y. Sun, *ACS Appl. Mater. Interfaces*, 2015, **7**, 8363.